Histochem Cell Biol (2005) 123: 377–392
DOI 10.1007/s00418-004-0743-4

ORIGINAL PAPER

Stavros I. Stavridis · Faramarz Dehghani
Horst-Werner Korf · Nils P. Hailer

Characterisation of transverse slice culture preparations of postnatal rat spinal cord: preservation of defined neuronal populations

Accepted: 26 November 2004 / Published online: 12 May 2005

Abstract Spinal cord injury induces degenerative and regenerative processes and complex interactions of neurons with non-neuronal cells. In order to develop an in vitro tool for the investigation of such processes, we prepared and characterised spinal cord slice cultures (SCSC) from Wistar rats (p0–12). SCSC were sustained in vitro up to 12 days and characterised by immunohistochemistry. Calbindin$^+$ neurons, distributed across the entire gray matter, were visible also after longer culture periods. NeuN$^+$ neurons were best preserved in the dorsal horn whereas large NeuN$^+$ and choline acetyltransferase$^+$ motoneurons in the ventral horn vanished after 3 days in vitro. Nestin immunoreactivity was found in animals of all age groups, either in cells interspersed in the ependymal lining around the central canal or in cells resembling protoplasmic astrocytes. Glial fibrillary acidic protein$^+$ astrocytes, initially restricted to the white matter, invaded the gray matter of SCSC early during the culture period. Microglial cells, stained by *Griffonia simplicifolia* isolectin B_4, were rapidly activated in the dorsal tract and in the gray matter but declined in number with time. SCSC derived from p0 or p3 animals showed a better preservation of the cytoarchitecture than cultures derived from older animals. In summary, SCSC undergo degenerative changes, but they contain defined neuronal populations, the cytoarchitecture is partially preserved and the glial reaction is limited.

S. I. Stavridis · N. P. Hailer
University Hospital for Orthopaedic Surgery Friedrichsheim, Johann Wolfgang Goethe-University, Frankfurt am Main, 60528 Federal Republic of Germany

S. I. Stavridis · F. Dehghani · H.-W. Korf
Institute of Anatomy II, Johann Wolfgang Goethe-University, Frankfurt am Main, 60590, Federal Republic of Germany

Present address: N. P. Hailer (✉)
Department of Orthopedics, Institute of Surgical Sciences, Karolinska Institute at Karolinska Hospital, 17176 Stockholm, Sweden
E-mail: nils.hailer@karolinska.se
Tel.: +46-8-51771516
Fax: +46-8-51774699

Keywords Slice culture · Spinal cord · Stem cells · Microglia

Introduction

Acute spinal cord injury is a complex two-step lesion involving mechanisms of primary and secondary damage. The immediate mechanical damage caused at the time of injury is followed by a sequence of cellular responses, including microglial and astrocyte activation. Microglia/macrophage activation and astrocyte hypertrophy are accompanied by the release of neurotoxins and cytokines, finally leading to the death of neurons and oligodendrocytes that were initially spared during the phase of primary damage. This cascade results in severe impairment of neuronal homeostatic mechanisms, axonal degeneration and demyelination (Tzeng et al. 2001). The only pharmacological agent known to ameliorate neurologic outcome in patients with spinal cord injury is methylprednisolone (Bracken 2002).

Organotypic cultures of the hippocampus or the cerebellum (Gähwiler 1984; Notterpek et al. 1993; Tauer et al. 1996) have become well established in in vitro models to study neuronal degeneration and regeneration. In some aspects, organotypic slice cultures are superior to in vivo models, as they combine organotypic tissue preservation with the advantage of easy visualisation and free access when pharmacological intervention is intended. In the present study, we prepared spinal cord slice cultures (SCSC) from postnatal rat spinal cord tissue in order to examine the reactions of distinct neuronal and glial populations. We analysed the influence of two parameters on tissue preservation in SCSC: (1) the animal age at the time of explantation, and (2) the duration of the in vitro period. In order to identify and distinguish neurons, astrocytes, microglial cells and precursor cells, we used well-established immunohistochemical markers:

(a) NeuN is a neuronal nuclear protein of 46–48 kDa apparently specific to neurons. Almost all neurons in the CNS and peripheral ganglia, with the exception of cerebellar Purkinje cells, mitral cells of the olfactory bulb and retinal photoreceptors, possess NeuN immunoreactivity. This distribution—together with the finding that glial cells lack NeuN immunoreactivity—makes NeuN a highly sensitive and specific marker of spinal cord neurons (Jansen et al. 1997; Manitt et al. 2001; Todd et al. 1998).

(b) Choline acetyltransferase (ChAT) is the enzyme responsible for the biosynthesis of acetylcholine. ChAT, a single-strand globular protein, is a specific marker of cholinergic neurons in the central and peripheral nervous system. Among many other locations, cholinergic neurons are found in the ventral horn of the spinal cord, representing motor neurons. As ChAT is synthesised in the perikaryon of cholinergic neurons and transported to the nerve terminals, it is present within cell bodies, dendrites, axons and axon terminals (Oda 1999; Phelps et al. 1984).

(c) Calbindin (CB), together with calretinin and parvalbumin, is a member of the family of calcium-binding proteins (CaBPs). CaBPs contribute to calcium homeostasis through their capacity to buffer cytosolic Ca^{++} and may also play a neuroprotective role when potentially dangerous increases in intracellular calcium concentration occur (Goodchild et al. 2000; Li et al. 1999; Magnusson et al. 1996; Ren et al. 1994). CaBPs often serve as a useful molecular marker for certain types of neurons, as each of them has been observed in different subsets of neurons (Celio 1990; Li et al. 2000). In the spinal cord, certain subsets of spinal interneurons (Antal et al. 1996) mainly in the dorsal horn (Albuquerque et al. 1999) and Renshaw cells in the ventral horn (Alvarez et al. 1999), display CB immunoreactivity.

(d) Glial fibrillary acidic protein (GFAP) is a 50-kDa protein and the principal 8–9 nm intermediate filament of astrocytes. It is rapidly upregulated in activated astrocytes and is therefore used as a marker to identify and characterise the reactions of astrocytes to CNS lesions (Kullberg et al. 2001; Morin-Richaud et al. 1998).

(e) *Griffonia simplicifolia* isolectin B_4 (IB_4) is a 114-kDa glycoprotein binding to galactose-containing glycoconjugates on cell membranes. In the CNS, it has a particularly strong affinity for microglial and perivascular cells, thus being a reliable marker for the detection of microglial cells (Prewitt et al. 1997; Stoll et al. 1999).

(f) Nestin is a large (200 kDa) intermediate filament protein abundantly produced in the cytoplasm of many multipotent precursor cells. Because it disappears as these cells differentiate, nestin is commonly used as a marker for CNS stem or progenitor cells (Kalman et al. 2001; Lendahl et al. 1990).

In this study, we characterise defined neuronal and glial populations over longer culture periods in SCSC from postnatal rat spinal cord, and we describe the reactions of these cell populations to in vitro culture.

Materials and methods

Wistar rats, p0–12, were raised and provided by the Zentrale Forschungseinrichtung of the Hospital of the Johann Wolfgang Goethe-University in Frankfurt am Main, Germany, according to the local guidelines for animal welfare. All experimental manipulations were performed under aseptic conditions using sterile instruments. After decapitation, the dorsal skin and musculature of the trunk were removed along the midline. A longitudinal laminectomy was performed from the cervical to the lumbar region of the vertebral column, the dura was opened and the spinal cord dissected from the denticulate ligaments and immediately placed in ice cold minimal essential medium (MEM, Gibco BRL Life Technologies, Karlsruhe, Germany) containing 1% glutamine (Gibco). The remnants of the surrounding dura mater spinalis were removed under microscopic control, and the spinal cord was cut into two segments: one cervicothoracic and one thoracolumbar. Both tissue segments were sandwiched between two agar blocks, providing mechanical stabilisation and reduced shear stress during sectioning. The spinal cord was cut into transverse slices of 400 µm using a sliding vibratome (Vibratome 1000 Classic, TPI St. Louis, MO, USA). From each spinal cord, 10–20 slices were obtained and transferred into cell-culture inserts (Becton Dickinson, Heidelberg, Germany; pore size 0.4 µm) that were placed in six-well culture dishes (Becton Dickinson). Two to three slices were placed in the same insert. Each well contained 1 ml culture medium consisting of 50% MEM, 25% Hank's balanced salt solution (HBSS; Gibco), 25% normal horse serum (NHS; Gibco), 2% glutamine, 1 µg/ml insulin (Boehringer, Mannheim, Germany), 2.4 mg/ml glucose (Braun, Melsungen, Germany), 0.1 mg/ml streptomycin (Sigma Chemicals, Taufkirchen, Germany), 100 U/ml penicillin (Sigma) and 0.8 µg/ml vitamin C (Sigma), pH = 7.4. The culture dishes were incubated at 35°C in a fully humidified atmosphere with 5% CO_2, and the culture medium was changed every second day.

After 0–12 days in vitro (div), SCSC were fixed with a mixture of 4% paraformaldehyde, 15% picric acid and 0.1% glutaraldehyde in 0.2 M phosphate buffer (PB) for 15 min, washed with 0.1 M PB and postfixed in the same fixative without glutaraldehyde for 3 h. SCSC were finally washed with 0.1 M PB for 1 h, carefully removed from the cell culture membrane and placed in 0.8 M sucrose solution containing 1.5% NaN_3. They were subsequently sectioned (14 µm) using a Microm HM 560 cryostat (Microm, Walldorf, Germany) at −19°C and mounted on gelatine-coated glass slides. After pretreatment with methanol and H_2O_2 (0.45%), the sections

were washed with 0.02 M phosphate-buffered saline (PBS) containing 0.3% Triton X-100 and incubated with normal horse serum (NHS, diluted 1:20 in PBS-Triton) for 30 min.

For immunohistochemical characterisation of the different cell populations, the following primary antibodies were used: (1) monoclonal mouse anti-NeuN (Chemicon, Hofheim TS, Germany), (2) monoclonal mouse anti-ChAT (Chemicon), (3) polyclonal rabbit anti-Calbindin (Dako, Hamburg, Germany), (4) monoclonal mouse anti-GFAP (Dako), (5) monoclonal mouse anti-nestin (Chemicon), and (6) biotinylated IB_4 (Sigma). SCSC were incubated with the primary antibody either for 24 h (NeuN, ChAT, CB, GFAP, nestin), or with biotinylated IB_4 for 1 h, diluted 1:100 (NeuN, ChAT), 1:400 (CB), 1:200 (GFAP), 1:1,000 (Nestin), or 1:20 (IB_4) in 0.02 M PBS containing 0.3% Triton with 5% bovine serum albumin (BSA, Sigma). After thorough washing with PBS-Triton (3×10 min), the secondary antibody [anti-mouse (Sigma) for NeuN, ChAT, GFAP and nestin, anti-rabbit (Sigma) for CB] was applied for 1 h, diluted 1:100 in PBS-Triton. Following repeated washing with PBS (3×10 min), preparations were incubated with avidin-biotin complex (Sigma, diluted 1:100 in PBS-Triton) for 1 h; 3,3′-diaminobenzidine (DAB; Sigma) was used as a chromogene. After washing with Tris-buffer (pH = 7.4), the sections were counterstained with hematoxylin, dehydrated through a graded series of ethanol and xylene and coverslipped with Entellan (Merck, Darmstadt, Germany).

For statistical analysis, the cell number of at least three samples from each group was counted using a light microscope, and mean numbers were calculated. The one-way ANOVA test was used to determine whether there were statistically significant differences in cell numbers among various groups, and $P < 0.05$ was considered significant. Subsequently, Bonferroni's adjustment for multiple comparisons was performed: for each age group, the 0 div group was set as the control group to which all others were compared.

Results

Distribution of neuronal and glial cell populations in immediately fixed spinal cord slices

The obvious macroscopically visible difference between cultures from the various age groups was in the size of the culture, as the diameter of the spinal cord increases proportionally with the age of the animal. In contrast, the immunohistochemical aspect of the acutely fixed preparations revealed, with the exception of nestin-immunoreactivity, no significant differences among various age groups.

$NeuN^+$ neurons were distributed across the entire spinal gray matter with almost no immunoreactivity seen in the white matter (Fig. 1a). In the head of the dorsal horn, smaller, round $NeuN^+$ neurons with a compact arrangement prevailed (Fig. 1c). In the neck and the base of the dorsal horn, the $NeuN^+$ cells appeared to be more loosely arranged and more heterogeneous in shape and size, with some of them being multipolar and considerably larger. The intermediate zone of the gray matter and the base of the ventral horn were generally occupied by loosely arranged neurons of varying size. In the head of the ventral horn, the larger motor neurons could be clearly recognised (Figs. 1b, 2b). The range of their soma sizes indicated that both larger α-motoneurons and smaller γ-motoneurons were present. They displayed strong NeuN immunoreactivity; this was strongest in the nucleus, weaker in the perikaryal cytoplasm and often extended into the proximal dendrites. These ventral horn motor neurons also demonstrated a strong ChAT-immunoreactivity (Fig. 2d). In the dorsal horn, the neurons were smaller and more densely packed than those in the adjacent area (Fig. 1c). Ependymal cells lining the central canal were not $NeuN^+$.

CB was distributed throughout the cytoplasm of neurons, and immunohistochemistry resulted in extensive staining of the dendritic trees that allowed for visualisation of the dendritic morphology. In general, CB immunoreactivity was distributed across the entire gray matter, but was also found in the white matter (Fig. 3a). The head of the dorsal horn displayed a strong CB immunoreactivity, with densely packed CB^+ structures that represented dendrites and axons and small, round cells forming a dense CB^+ band in the superficial dorsal horn. CB^+ neurons constituted a morphologically homogeneous population of smaller neurons, some of which gave rise to stained dendrites or processes. The ventral horn harboured a dense network of CB^+ fibres (Fig. 3b). Many medium- to large-sized neurons with long processes were frequently found (Fig. 3d). Large numbers of CB^+ fibres were found in the funiculi of the spinal cord white matter, with the highest density of CB^+ fibres found in the dorsolateral funiculus while the pyramidal tract did not contain labelled fibres. Ependymal cells lining the central canal displayed a strong CB immunoreactivity, with the most prominent immunoreactivity being found ventrally and dorsally to the central canal. At the dorsal aspect of the spinal canal, a cluster of CB^+ cell bodies and fibres could be observed, and many of the CB^+ fibres crossed the mid-line dorsally.

Glial fibrillary acidic protein immunoreactivity was most prominent in the white matter (Fig. 4a). Astrocytes of the external membrane were strongly stained by the anti-GFAP antibody, and most white matter astrocytes showed the typical radial organisation, which was more prominent in the ventral and lateral portions of the white matter. The predominant astrocyte was radially oriented and appeared to span the white matter from the pial surface to the interface between the gray and white matter (Fig. 4b). GFAP immunoreactivity was barely detectable in the gray matter, where only few $GFAP^+$

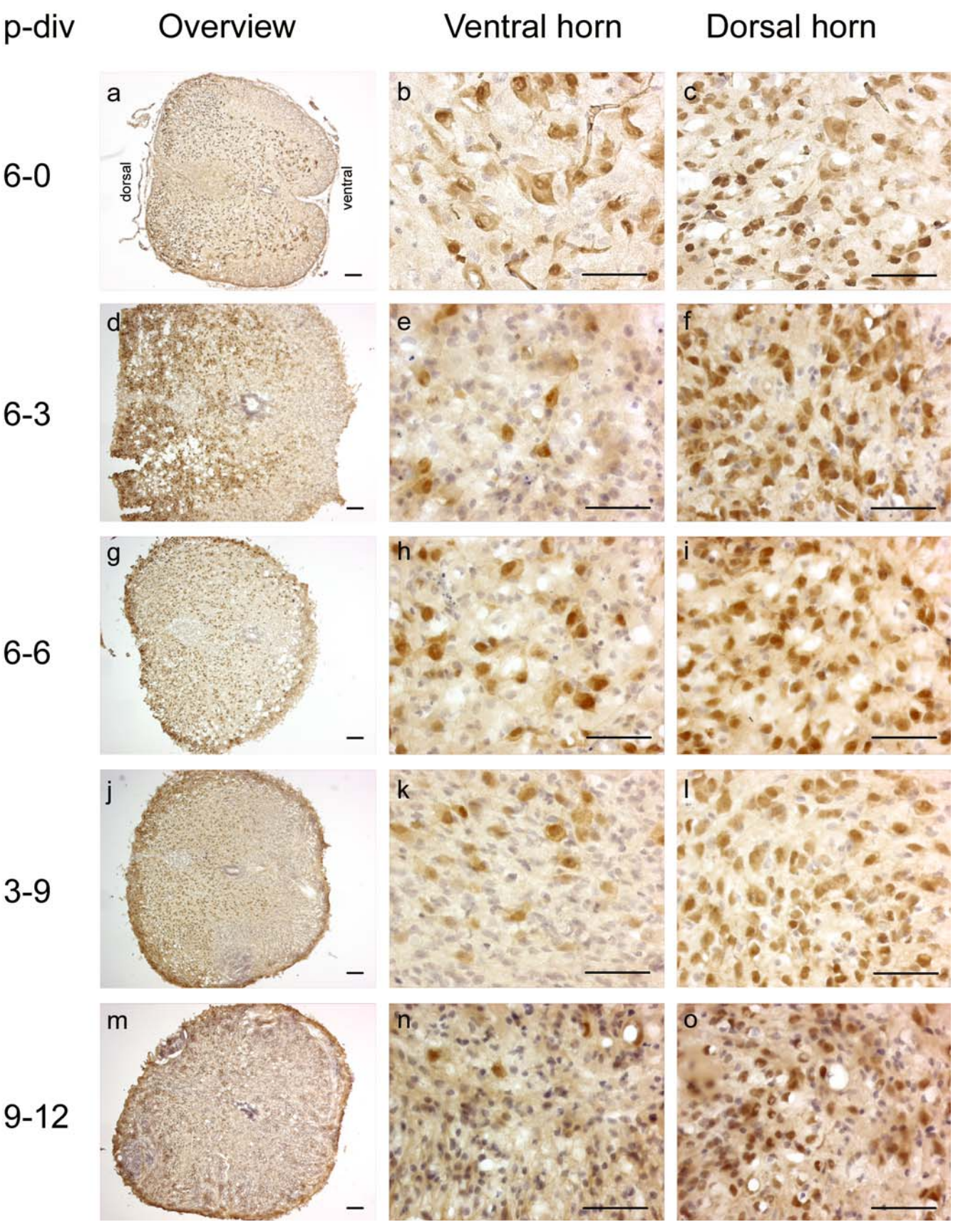
p-div
Overview
Ventral horn
Dorsal horn
6-0
6-3
6-6
3-9
9-12
a
b
c
d
e
f
g
h
i
j
k
l
m
n
o
dorsal
ventral

◀

Fig. 1 NeuN immunoreactivity in spinal cord slice cultures (SCSC). In SCSC fixed immediately after explantation [0 days in vitro (div)], $NeuN^+$ neurons are distributed across the entire spinal cord gray matter (**a**). Larger motoneurons are situated in the ventral horn and display strong NeuN immunoreactivity (**b**). Smaller, round neurons in the dorsal horn are also $NeuN^+$ (**c**). After 3 div, the larger motoneurons of the ventral horn are no longer stained (**d**, **e**). In contrast, other ventral horn neuronal populations (**e**, **h**) and dorsal horn neurons (**f**, **i**) are well preserved after 3 div (**d–f**) and 6 div (**g–i**). After longer culture periods, neurons remain well preserved both in cultures derived from younger animals (**j–l**) and from older animals (**m–o**), with the former displaying a better quality of tissue preservation and larger numbers of $NeuN^+$ neurons. "p-div" refers to the age of the animal at the age of explantation (*p*) and the number of days in vitro (*div*). *Scale bars* in all figures: 100 μm

Fig. 2 Choline acetyltransferase (ChAT) immunoreactivity in spinal cord slice cultures (SCSC). In acutely fixed SCSC [0 days in vitro (div)], the $NeuN^+$ motoneurons around the central canal (**a**, **b**) display strong ChAT immunoreactivity (**c**, **d**). After 3 div, the number of the $ChAT^+$ motor neurons is reduced, as is the intensity of the remaining ChAT immunoreactivity (**e–h**). After 6 div, ChAT immunoreactivity in the ventral horn is barely detectable (**i–l**), demonstrating the early prominent degeneration of the $ChAT^+$ motoneurons. "p-div" refers to the age of the animal at the age of explantation (*p*) and the number of days in vitro (*div*). *Scale bars* in all figures: 100 μm

astrocytes were visualised, presenting a small, stellate perikaryon and thin, branched processes (Fig. 4c). Central canal ependymal cells were devoid of GFAP immunoreactivity.

IB_4 staining was very weak in immediately fixed slices (Fig. 5a, b) where it was most prominent in the spinal capillaries. A very limited number of IB_4^+ microglial cells without specific spatial distribution were observed. These cells almost exclusively exhibited an amoeboid morphology with round or elongated somata. Only few cells had developed one or two very small, mainly unbranched processes. Virtually no microglial cells that displayed the typical ramified, "resting-state" morphology were found.

The only difference between different age groups observed in acutely fixed cultures concerned nestin immunoreactivity: in slices fixed immediately after explantation and derived from p0 to p6 animals, white matter nestin immunoreactivity was mainly localised in the ventral and lateral portions (Fig. 6a). The pial surface displayed an increased nestin immunoreactivity. Long, radially oriented arborising processes ran from this region towards the interface between the white and gray matter (Fig. 6b). The pattern was almost identical to that of GFAP immunoreactivity seen in the white matter. Some scattered $nestin^+$ elements resembling

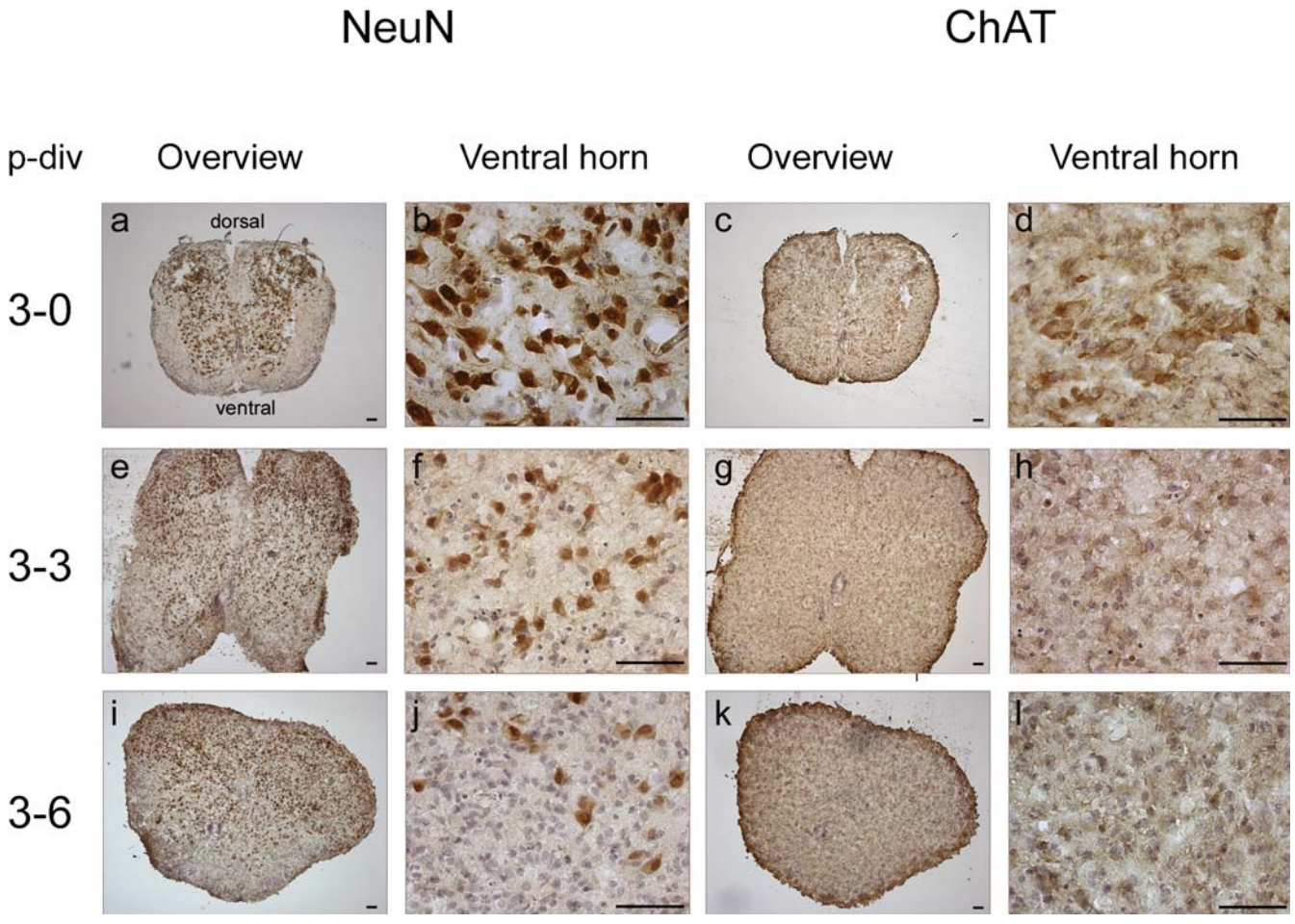

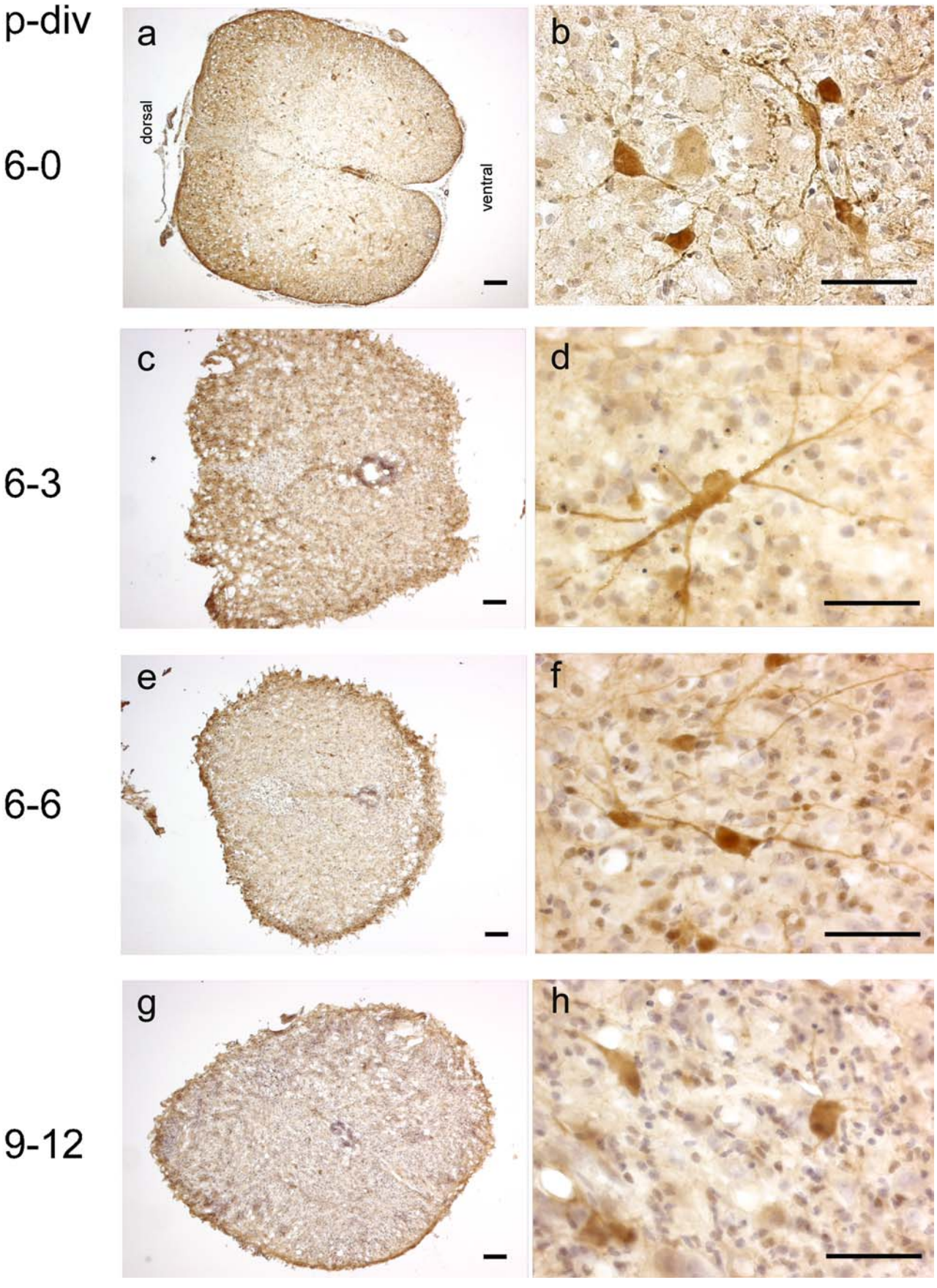
p-div
6-0
6-3
6-6
9-12
a
b
c
d
e
f
g
h
dorsal
ventral

◀

Fig. 3 Calbindin (CB) immunoreactivity in spinal cord slice cultures (SCSC). CB immunoreactivity is found both in the gray and the white matter of the spinal cord fixed immediately after explantation, with the superficial dorsal horn demonstrating strong CB immunoreactivity (**a**). Large CB^+ neurons are found in the ventral horn (**b**). After 3 days in vitro (div) (**c**, **d**) or 6 div (**e**,**f**), the pattern of CB immunoreactivity remains well preserved in the superficial dorsal horn. Renshaw cells in the ventral horn (**d**) and other large CB^+ neurons scattered across the gray matter are accompanied by a dense network of immunoreactive axons and dendrites (**f**). Ependymal cells are also CB^+ (**c**, **e**). After longer culture periods, CB^+ neurons are well preserved, even in SCSC derived from older animals (**g**, **h**). CB immunoreactivity around the central canal remains elevated (**g**). "p-div" refers to the age of the animal at the age of explantation (*p*) and the number of days in vitro (*div*). *Scale bars* in all figures: 100 μm

protoplasmic astrocytes were found in the gray matter. Around the spinal canal, increased nestin immunoreactivity was observed. Ependymal cells lining the spinal canal were $nestin^+$, with the most profound signal localised in the ventral and dorsal ependymal cells from which $nestin^+$ processes were observed to spread towards the gray matter and to reach the ventral and dorsal border of the spinal cord (Fig. 6c). This pattern closely resembled the pattern of the CB immunoreactivity around the central canal. Labelling of blood vessels was also found in immediately fixed slices, but it disappeared with prolonged culture periods. In contrast, in older animals (p9 or p12), nestin immunoreactivity was significantly less intense (Fig. 6j–l).

The spatiotemporal reaction pattern of neurons and glial cells in SCSC during culture

Overall, cultures derived from younger animals (p0 or p3) appeared to be better preserved than those derived from older animals (p9 or p12). With prolonged culture time, there was a gradual degradation in tissue quality and cytoarchitecture preservation, appearing mainly in the form of vacuolisation and being more severe in the outer borders of the white matter. The most prominent alterations, however, occurred during the first 3 div.

Early motor neuron death

Already after 3 div, the larger motoneurons originally situated in the ventral horn and displaying a strong NeuN and ChAT immunoreactivity (Fig. 2a–d) began to show signs of degeneration (Figs. 1e and 2e–h). The number of the $ChAT^+$ motor neurons was reduced, as was the intensity of the remaining ChAT immunoreactivity. This was accompanied by a slight decrease in the number of $NeuN^+$ neurons, but many neurons continued to display strong NeuN immunoreactivity and a healthy morphological phenotype (Fig. 1h). The $NeuN^+$ cells in the dorsal horn appeared to be well preserved; there was no significant reduction in their numbers or alteration of their morphology (Fig. 1f, i). After 6 div, ChAT immunoreactivity in the ventral horn was barely detectable, and NeuN immunoreactivity was further reduced. After prolonged culture periods (9–12 div), the pattern of NeuN immunoreactivity remained mainly unchanged in younger animals (p0–6): a decrease in the total amount of $NeuN^+$ cells was observed in the ventral horn while in the dorsal horn, the number of $NeuN^+$ neurons remained largely unchanged although some signs of degeneration could be detected (Fig. 1j–l, Table 1). Longer culture periods (9–12 div) in older animals (p9–12) induced a statistically significant reduction in the number of $NeuN^+$ cells in both the ventral and dorsal horns (Table 1), but a large amount of $NeuN^+$ cells remained visible in the dorsal horn (Fig. 1m–o).

CB^+ neurons persist in SCSC

After 3–6 div, CB immunoreactivity in the dorsal horn was well preserved (Fig. 3c, e), especially in younger animals. Some of the dorsal horn CB^+ neurons gave rise to stained dendrites or processes. Many large ventral horn CB^+ cells remained intact, showing a healthy morphology and strong CB immunoreactivity with robust staining of their dendritic trees (Fig. 3d). The dense network of CB^+ fibres also remained clearly visible (Fig. 3f). With prolonged time in vitro, CB immunoreactivity appeared to increase in the ependymal cells lining the spinal canal. The cluster of CB^+ cell bodies and fibres, located at the dorsal aspect of the central canal, appeared to expand with prolonged culture periods, and the CB^+ fibre zone that crossed the mid-line dorsally became more prominent. Generally, even after prolonged culture periods (9–12 div), CB immunoreactivity appeared well preserved in both the gray and the white matter although a significant reduction in the total number of CB^+ neurons did occur after 9 div in younger animals and after 3–6 div in older animals (Fig. 3g–h).

GFAP immunoreactivity increases in SCSC early during the culture period

After 3 div, a strong increase in GFAP immunoreactivity was observed (Fig. 4d). $GFAP^+$ astrocytes, initially restricted almost exclusively to the white matter, were now found in large numbers in the gray matter. In the white matter, there was a slight increase in the staining of the processes of the radial cells (Fig. 4e). Although the typical radial organisation of the white matter astrocytes was in many cases less apparent, their total number demonstrated no significant alteration throughout longer culture periods (Table 1). The most prominent increase in GFAP immunoreactivity was observed in the gray matter. Already after 3 div, a sta-

Fig. 4 Glial fibrillary acidic protein (GFAP) immunoreactivity in spinal cord slice cultures (SCSC). In the spinal cord fixed immediately after explantation, GFAP immunoreactivity is almost exclusively restricted to the white matter (**a**). Astrocytes are oriented radially, spanning the white matter from the pial surface to the interface between gray and white matter (**b**). Only few astrocytes are present in the gray matter (**c**). After 3 days in vitro (div) (**d**), GFAP immunoreactivity remains detectable in the white matter (**e**) while it is clearly elevated in the gray matter (**f**). After 6 div (**g**–**i**) and 9 div (**j**–**l**), the number of white matter astrocytes remains elevated (**h**, **k**), and the gray matter further displays numerous strong $GFAP^+$ astrocytes (**i**, **l**). ''p-div'' refers to the age of the animal at the age of explantation (*p*) and the number of days in vitro (*div*). *Scale bars* in all figures: 100 μm

Fig. 5 *Griffonia simplicifolia* isolectin B_4 (IB_4) immunoreactivity in spinal cord slice cultures (SCSC). In the spinal cord investigated immediately after explantation, almost no IB_4 immunoreactivity can be found, apart from blood vessels (**a**, **b**). In the course of in vitro culture, IB_4^+ microglial cells are found predominately in the corticospinal tract and in the white matter (**c**, **e**). Some ramified, ''resting-state'' microglial cells are scattered across the white and gray matter (**d**) while the majority of microglial cells demonstrate the round or amoeboid shape typical of ''activated'' microglia (**d**, **f**). After longer culture periods, fewer IB_4^+ cells can be found (**g**, **h**). ''p-div'' refers to the age of the animal at the age of explantation (*p*) and the number of days in vitro (*div*). *Scale bars* in all figures: 100 μm

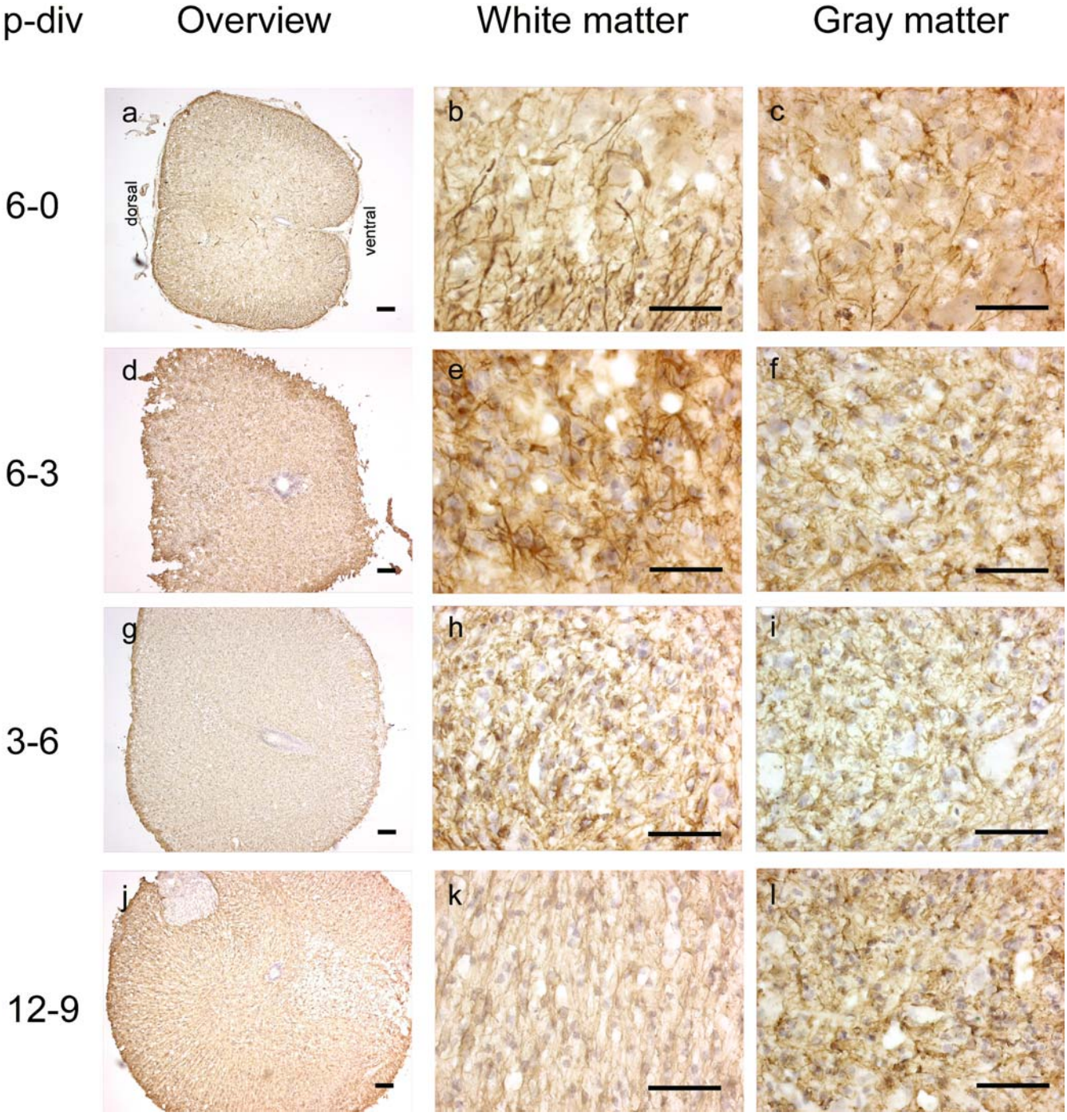

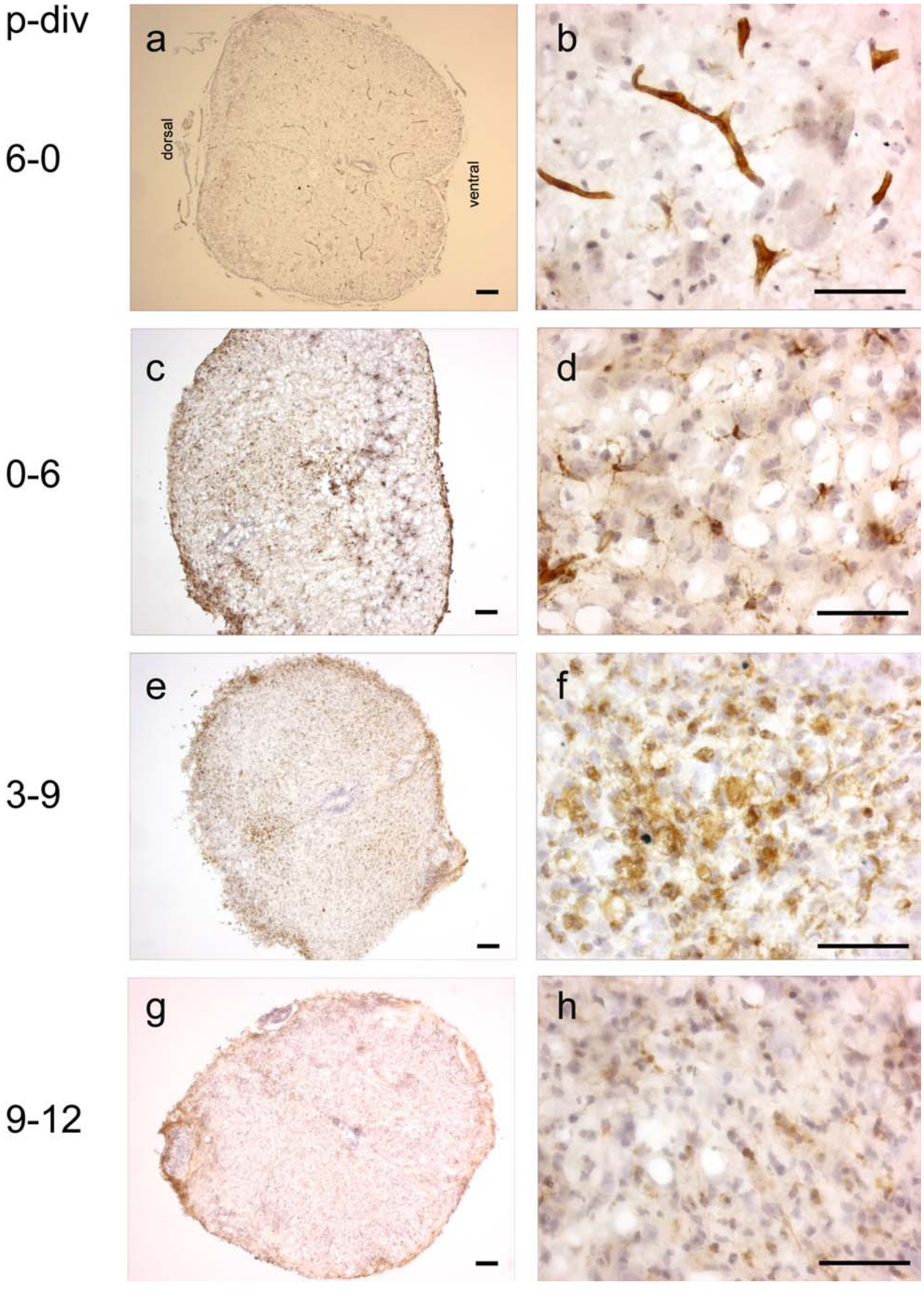
p-div
6-0
0-6
3-9
9-12
a
b
c
d
e
f
g
h
dorsal
ventral

tistically significant increase in the number of gray matter GFAP$^+$ astrocytes was observed in both younger and older animals, and it remained elevated for the remaining culture period (Table 1). Gray matter astrocytes appeared tightly packed and hyperfilamentous and displayed thick, richly branched, strongly immunoreactive processes (Fig. 4f). After longer culture periods (6–12 div, Fig. 4g–l), GFAP immunoreactivity remained high in both white (Fig. 4h, k) and gray (Fig. 4i, l) matter without signs of alteration in the morphology of GFAP$^+$ astrocytes.

IB_4 immunoreactivity increases in the white matter

After 3 div, IB_4 immunoreactivity increased mainly in the dorsal tract, in the ventral and lateral portions of the white matter and at sites of focal tissue destruction (Fig. 5c–f). Two morphologically distinct forms of microglial cells were observed, representing the "resting" and the "activated" states: the former exhibited a ramified morphology, displaying multiple long, richly branched processes, and was found scattered across the entire spinal cord both in the white and the gray matter (Fig. 5d). The latter phenotype was overwhelmingly found in the white matter and demonstrated large somata with round or amoeboid morphology (Fig. 5f). There was a considerable increase in cell size and staining intensity when compared with the microglial cells found in immediately fixed slices and those scattered in the gray matter. The highest IB_4 immunoreactivity was typically found in the dorsal part of the corticospinal tract in a relatively well-defined area where the majority of microglial cells displayed a large, round cell soma and large phagocytic vacuoles representative of the activated microglial state (Fig. 5f). Quantitatively, the number of microglial cells reached its peak between 3 div and 6 div and declined after longer culture periods (9 div; Fig. 5g, h; Table 1).

Nestin immunoreactivity persists in vitro and is found in cells lining the central canal

After 3 div, an upregulation of nestin immunoreactivity occurred. Numerous strongly immunoreactive processes extended from the pial surface and spread across the entire spinal cord white matter, even entering the gray matter. The increase was more prominent in SCSC derived from older animals (p9 or p12; Fig. 6m, n) since these demonstrated only weak nestin immunoreactivity in acutely fixed slices (Table 1). The gray matter contained a relatively low number of nestin$^+$ structures that resembled protoplasmic astrocytes. Nestin expression in ependymal cells remained elevated, especially in p0–6 animals, and a plexus of nestin$^+$ fibres extending towards the gray matter that surrounded the central canal was observed (Fig. 6f, i). This plexus was more intensely labelled in the slices derived from younger animals (p0–6). In slices from older animals (p9 or p12), the increase of nestin immunoreactivity prevailed in the white matter (Fig. 6n, q), and only weak nestin immunoreactivity was found around the central canal (Fig. 6o, r). In summary, in slices derived from p0, p3 or p6 animals, nestin immunoreactivity remained high or was even upregulated in both the white matter and in the gray matter around the spinal canal (Fig. 6d–i). In slices derived from p9 or p12 animals, there was a significant, early, long-lasting upregulation of nestin immunoreactivity in the white matter while it was less intense around the central canal (Fig. 6m–r). With prolonged culture time, the nestin immunoreactivity was not significantly reduced.

Fig. 6 Nestin immunoreactivity in spinal cord slice cultures (SCSC). In the spinal cord derived from younger animals (p0 or p3) and fixed immediately after explantation, nestin immunoreactivity is prominent (**a**), with radially oriented nestin$^+$ cells in the white matter (**b**). Ependymal cells are nestin$^+$, and there is a bundle of nestin$^+$ cells and fibres spreading towards the ventral and dorsal aspect of the spinal cord (**c**). In SCSC derived from younger animals and cultured for 6 days in vitro (div) (**d**–**f**) or 9 div (**g**–**i**), nestin expression remains elevated in the white matter (**e**, **h**) and especially around the central canal (**f**, **i**). In the spinal cord derived from older animals (p6 or p12; **j**–**l**) only weak nestin immunoreactivity can be found in the white matter (**k**) and around the central canal (**l**) after 6 div or 9 div. In SCSC derived from older animals (p6 or p12), there is a rapid, robust, and long-lasting increase in nestin expression, predominately in the white matter (**n**, **q**) and less around the central canal (**o**, **r**). "p-div" refers to the age of the animal at the age of explantation (*p*) and the number of days in vitro (*div*). *Scale bars* in all figures: 100 μm

Discussion

In this study, we investigated SCSC derived from rats of different ages in order to examine the suitability of these preparations as an in vitro model for degenerative and regenerative reactions after spinal cord injury. Slice cultures from other regions of the CNS can be maintained in vitro for several weeks, and cells within such preparations preserve the tissue-specific cell connections that exist in vivo, as well as local neuronal circuits with the appropriate patterns of innervation. The combination of pharmacological accessibility and long-term survival along with the preservation of regional differentiation, neuroanatomic organisation and cell-to-cell interaction renders organotypic slice cultures a very useful model in the study of neuronal tissue (Bernaudin et al. 1998).

The number, morphology and distribution of smaller NeuN$^+$ neurons in the gray matter of SCSC appear to remain well preserved, even after prolonged culture periods. CB$^+$ neurons show a capacity for survival over prolonged culture periods although their numbers decline significantly. The majority of CB$^+$ neurons in the dorsal horn presumably represented local interneurons (Nazli et al. 2000) whereas in the ventral horn, the medium- to large-sized CB$^+$ neurons with long

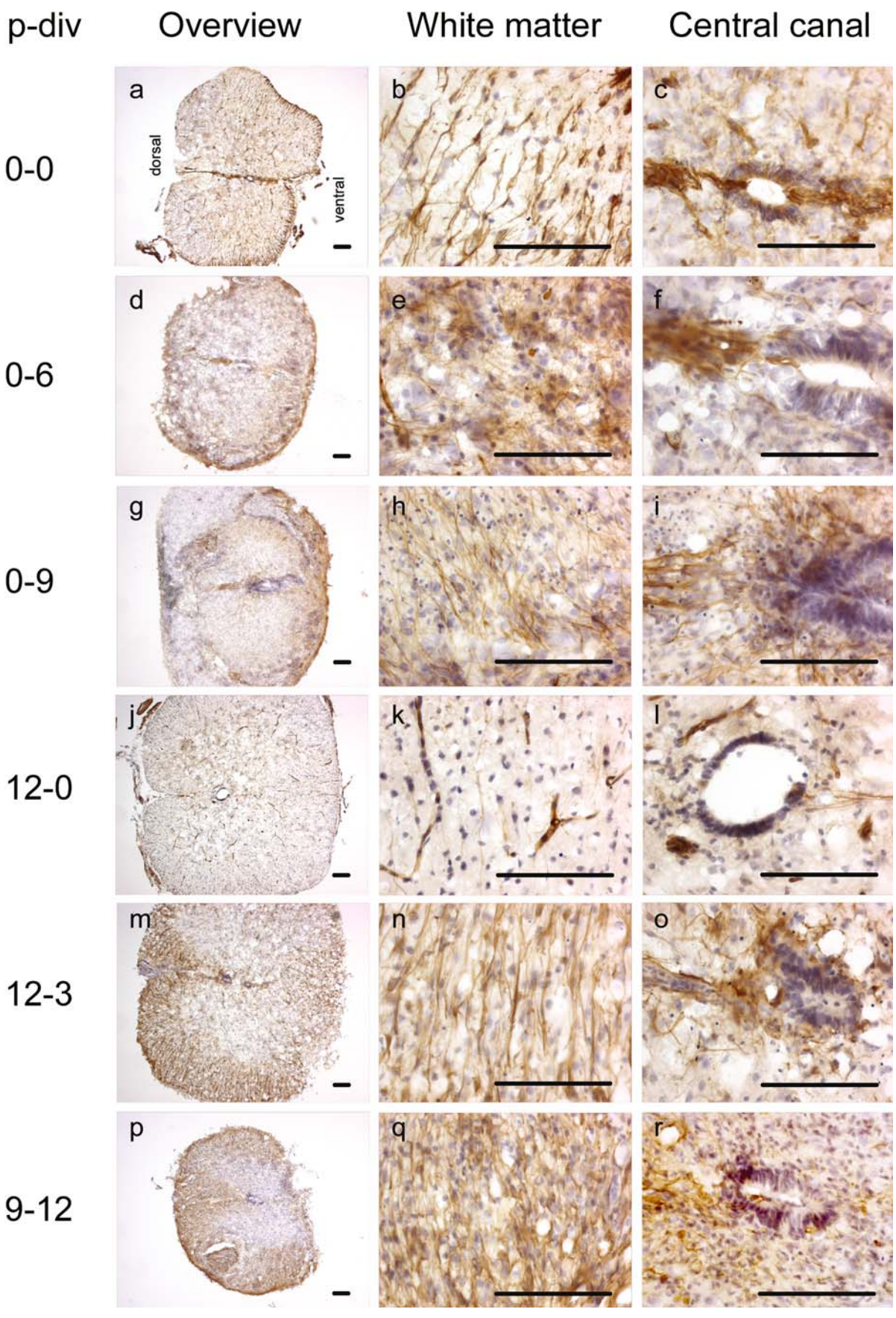
p-div
Overview
White matter
Central canal
0-0
0-6
0-9
12-0
12-3
9-12
a
b
c
d
e
f
g
h
i
j
k
l
m
n
o
p
q
r
dorsal
ventral

Table 1 Quantitative evaluation of the numbers of cells positive for NeuN, calbindin (CB), glial fibrillary acidic protein (GFAP), *G. simplicifolia* isolectin B_4 (IB_4), and nestin.[a] *div* days in vitro, *p0, p6, p9* age of animals at time of tissue explantation, *v.h* ventral horn, *d.h* dorsal horn, *w.m* white matter

[a] Mean numbers ± standard deviations are indicated
*$P < 0.05$; **$P < 0.01$; ***$P < 0.001$

	0 div	3 div	6 div	9 div
NeuN				
p0				
v.h.	95 ± 5.7	89.5 ± 4.63	91.25 ± 2.02	51 ± 5.2**
d.h.	319.5 ± 6.41	306 ± 7.76	283.5 ± 21.4	255.7 ± 3.53
p6				
v.h.	69.67 ± 4.06	62 ± 1	48 ± 2.65	25.67 ± 2.91**
d.h.	252.3 ± 6.39	260.5 ± 1.5	231.3 ± 12.67	250.8 ± 20.72
p9				
v.h.	94 ± 9.24	61.5 ± 1.5	23 ± 2***	12.25 ± 0.48***
d.h	292.7 ± 3.49	193 ± 7	162.5 ± 18.5**	123.3 ± 20.95***
CB				
p0	73 ± 7.57	63 ± 2	44 ± 2.78	39.25 ± 2.66*
p6	75 ± 5.03	79 ± 7	44.67 ± 4.41	31 ± 7.43***
p9	89 ± 6.25	42 ± 1**	48 ± 3.79**	20 ± 2.74***
GFAP				
p0				
w.m.	33.67 ± 0.88	30 ± 1	30 ± 3.79	31 ± 1.16
g.m.	5.33 ± 0.88	31 ± 2.31*	29 ± 2.08*	31.33 ± 2.19*
p6				
w.m.	47.6 ± 2.87	43.75 ± 2.27	41.75 ± 1.55	39 ± 0.71
g.m.	21.2 ± 1.72	65.63 ± 3.27***	63.67 ± 4.36***	70 ± 5.29***
p9				
w.m.	39.33 ± 1.45	33.67 ± 0.88	34.67 ± 2.4	33.67 ± 1.76
g.m.	23.67 ± 1.33	65 ± 4.62***	77 ± 3.46***	92.33 ± 2.03***
IB_4				
p0	16.33 ± 2.33	183.5 ± 12.5***	80.5 ± 11.65*	56.67 ± 6.49
p6	17 ± 1.53	141.2 ± 17.01***	71.6 ± 4.4	45.4 ± 4.21
p9	24 ± 1.15	72.33 ± 9.94	124.2 ± 6.89***	67.8 ± 8.25
Nestin				
p0	27 ± 1.15	18.8 ± 1.78	15 ± 1.73	10.5 ± 0.64***
p6	12.33 ± 0.88	35.25 ± 3.68***	17 ± 1.58	15.33 ± 2.33
p9	7.5 ± 0.5	27 ± 1**	17 ± 1	13.5 ± 1.5

processes were suspected to be Renshaw cells (Carr et al. 1998; Ren et al. 1994). CB is a member of the EF-hand family of CaBPs. It has been proposed that, because of their calcium-buffering capacity, these proteins may protect neurons against potentially harmful increases in intracellular calcium ions (D'Orlando et al. 2001; Iacopino et al. 1992; McMahon et al. 1998; Rintoul et al. 2001). Abnormally high and sustained increases in the intracellular calcium ion concentration ($[Ca^{2+}]_i$) may activate catabolic enzymes, including protein kinase C, calpains, phospholipase A_2, nitric oxide synthase and endonucleases, the consequence of which is necrotic or apoptotic cell death. As the increase in $[Ca^{2+}]_i$ plays a key role in excitotoxic cell death, neurons that express CB or the other CaBPs may be more resistant than those that do not. After unilateral spinal nerve transsection in p3 rats, no loss of cells was found among CB^+ neurons after 3 days and 18 days (Lim et al. 2000).

In contrast to this relatively high degree of preservation of smaller $NeuN^+$ or CB^+ neurons, SCSC demonstrate a significant and early loss of large motoneurons in the ventral horn. Already after 3 div, these $NeuN^+$ and $ChAT^+$ neurons display strong signs of degeneration accompanied by a large reduction of ChAT immunoreactivity although other $NeuN^+$ and CB^+ ventral horn neurons are still present. It has been argued that targets and afferents interact in the control of neuronal survival (Oliveira et al. 2002). Target deprivation of immature motoneurons results in massive neuronal death, especially in the first days of postnatal life (Chan et al. 2002; Greensmith et al. 1996). However, this susceptibility declines during the first 2 weeks of postnatal development, and developing motoneurons begin to express a regenerative capacity up to p14 (Chan et al. 2002). Unilateral spinal nerve transsection in p3 rats results in a marked reduction in the number of ventral horn motoneurons compared with the un-lesioned side after 3 days (Lim et al. 2000). Similarly, after root avulsion in neonates, a rapid, massive loss of spinal motoneurons occurs (Wu et al. 1995; Yuan et al. 2000). In a model of spinal contusion injury, the loss of large ventral horn neurons adjacent to the thoracic injury site is extensive 24 h after spinal cord injury, with no evidence of significant additional loss 1 month later (Grossman et al. 2000; Grossman et al. 2001). Taken together, the early loss of ventral horn motoneurons observed in our slice cultures correlates well with the observation that immature motoneurons are vulnerable to target deprivation. Moreover, this loss of a defined neuronal population seems to follow a general reaction pattern of "organotypic" slice culture preparations: even in the well-established entorhinal–hippocampal slice culture model, in which defined hippocampal neuronal populations persist, great neuronal loss is observed in the hippocampal formation and in adjacent cortical regions (Pozzo-Miller et al. 1994).

GFAP immunoreactivity follows an interesting spatiotemporal reaction pattern. While in immediately fixed slices it is found almost exclusively in the white matter, reactive astrocytes begin to appear in the gray matter after 3 div. In vivo, after a C2 spinal cord hemisection, changes in astrocyte morphology and increase in GFAP immunoreactivity were observed within 1 h and persisted (Hadley et al. 1997). In a spinal cord transsection study, there was an upregulation of GFAP mRNA within 30 min that persisted up to 3 days after the injury while the increase of GFAP immunoreactivity peaked after 3 days and remained high in both gray and white matter after 1 week (Morin-Richaud et al. 1998). This upregulation of GFAP immunoreactivity is one of the hallmarks of "reactive astrogliosis" or "glial scarring". Reactive astrogliosis is the CNS response to a variety of harmful stimuli, such as trauma or ischemia. The end result is a scar tissue consisting of tightly packed hyperfilamentous astrocytes (Fawcett et al. 1999; Ridet et al. 1997). In SCSC, this astrogliosis, however limited it may be, has to be considered as an indicator of degenerative changes.

IB_4^+ microglial cells are resident CNS macrophages that play an important role after injury. Immediately fixed spinal cord slices contain a very limited number of IB_4^+ cells. The majority of these are seen close to the remnants of spinal capillaries, possibly representing perivascular microglia. Very few resting ramified cells and some cells with an ovoid or amoeboid soma and short processes are found scattered across the gray and white matter with no specific distribution pattern, which is in accordance with earlier observations (Stoll et al. 1999). After 3 div, there is a striking increase in the number of microglial cells at sites of focal tissue destruction, the white matter and mainly the dorsal corticospinal tract, reflecting the clearance of degenerating descending axons by activated microglia. The number of microglial cells remains elevated after 6 div, but their number seems to decrease after prolonged culture periods (9–12 div). It is well known that following CNS injury a rapid activation and proliferation of microglial cells occurs but that numbers and degree of microglial activation decrease—sometimes even to control levels—with time (Hailer et al. 1999; Rabchevsky et al. 1997). In the developing CNS, primordial microglia have a rounded or amoeboid morphology, and as the CNS matures, these amoeboid microglia differentiate into increasingly ramified cells (Streit et al. 1999). Our observation that most microglial cells found in acutely fixed slices display an amoeboid morphology may reflect the immature state of these cells in cultures derived from animals 12 days of age or younger.

Following brain or spinal cord injury, cellular hypertrophy of microglial cells is apparent after 24 h. Microglial cells begin to proliferate 2–3 days after injury, their numbers reach maximal levels after 4–7 days and usually subside at later time points. This pattern has been described in most experimental models: after dorsal hemisection, dorsal root lesion or sciatic nerve injury, proliferation and recruitment of macrophages and microglial cells become predominant 2 days after the injury, and their density at the lesion site is maximal between 4 days and 8 days after a lesion (Dusart et al. 1994; Liu et al. 2000). In a spinal contusion model, microglial cells were present after 24 h, predominantly located within the gray matter and dorsal funiculus white matter (Carlson et al. 1998). Peak numbers were observed between 3 days and 7 days post-injury (Popovich et al. 1997). In most spinal cord lesion models, microglial activation was not confined to the lesion site but was also observed in distal regions (Carlson et al. 1998; Leme et al. 2001). In a comparative experimental model, the extent and severity of the inflammatory reaction in the spinal cord greatly exceeded that seen in the brain at all time points analysed (Schnell et al. 1999).

In SCSC, the spatiotemporal reactivity pattern of IB_4-immunoreactive cells largely correlates with that found in vivo. The increased IB_4 immunoreactivity and the microglial cell morphology observed in the white matter and especially in the dorsal corticospinal tract reflect microglial phagocytic activity initiated by demyelination and degeneration of axons belonging to the interrupted spinal tracts. This reaction remains limited, affecting defined regions and subsiding after some time.

Nestin immunoreactivity displays a pattern similar to GFAP immunoreactivity in the white and gray matter while in an area around the central canal it resembles CB immunoreactivity. Nestin, a cytoskeletal embryonic intermediate filament, belongs to class III intermediate filaments that also include vimentin and GFAP (Wei et al. 2002). Nestin appears prenatally in immature cells of neuroepithelial origin, such as neuroepithelial columnar cells, radial glia, multipotent stem cells, bipotential glial/neuronal progenitor cells, oligodendroglia-type2-astrocyte progenitor cells, pro-oligodendrocytes and maturing astrocytes (Kalman et al. 2001). Nestin is downregulated either at the onset of GFAP or neurofilament expression or during subsequent differentiation of multipotential neural precursor into astrocytes or neurons. The transient abundant expression of nestin is considered a marker for neural precursor cells in the developing CNS of mammals (Wei et al. 2002). In postnatal rat spinal cord, the nestin gene was found to be downregulated after postnatal day 6 (Dahlstrand et al. 1995; Schmidt-Kastner et al. 2002). This is in accordance with our observation of decreased nestin expression in cultures derived from p9 or p12 animals.

Experiments on the adult rat spinal cord have demonstrated that some ependymal cells lining the spinal canal are neural stem cells (Johansson et al. 1999). However, others have suggested that neural progenitors are distributed throughout the parenchyma in the adult spinal cord and are not ependymal cells (Yamamoto et al. 2001). Findings concerning nestin upregulation in a spinal cord injury model suggest that there are two possible sources of precursor cells in the adult spinal cord: astrocytes on the pial surface and ependymal cells. It is known that nestin expression is

increased in reactive astrocytes forming the glial scar in both the white and the gray matter (Frisen et al. 1995). After traumatic brain injury in the rat, the expression of nestin was not confined to astrocytes, but IB_4^+ microglia/macrophages also expressed nestin (Sahin et al. 1999). In addition to reactive astrocytes, nestin is induced in CB^+ ependymal cells following injury. This induction begins soon after injury, and at later time points, nestin-expressing cells and fibres are also found further distant from the central canal (Frisen et al. 1995; Shibuya et al. 2002). The nestin signal in the ependymal cells was stronger near the injury site, but it was also found remote from the injury site. The time pattern of nestin immunoreactivity upregulation was similar in most injury models: it started during the first 24 h, reached a peak after 7 days, remained elevated and decreased slowly up to the fourth week (Liu et al. 2002; Sahin et al. 1999; Shibuya et al. 2002). This nestin re-expression in adult astroglial cells implies that these cells retain—to a certain extent—the state of embryonic precursor cells, and may be involved in neurogenesis and reparative processes in the CNS.

In SCSC derived from p0, p3 or p6 animals, nestin expression was elevated compared with preparations from p9 or p12 animals. The initial pattern of nestin immunoreactivity is in accordance with the presence of neuronal stem cells in the ependymal layer and the subpial astrocyte layer, as these are the sites of the major nestin immunoreactivity. It also illustrates the plasticity of young postnatal astrocytes that maintain high nestin levels. The obvious overlap between nestin, GFAP, and CB immunoreactivity observed in our slice culture model supports the idea that $GFAP^+$ astrocytes and CB^+ ependymal cells are the main sources of nestin expression. Moreover, the pattern of nestin upregulation in our culture model at later time points and the re-expression of nestin in cultures derived from older animals are in accordance with in vivo models of spinal cord injury.

In summary, it was our aim to investigate the possibility of establishing an in vitro model that permits the study of degenerative and regenerative reactions after spinal cord lesions. We provide evidence that in vitro culture of postnatal rat spinal cord is possible; as defined, neuronal and glial populations remain preserved over a culture period of at least 9 div. The preservation of distinct neuronal populations indicates that some of them are little affected by the unavoidable interruption of most afferent and efferent neuronal pathways since local neuronal circuitries and cell-to-cell interactions remain preserved inside the slice cultures. On the other hand, the early loss of $ChAT^+$ motoneurons and other large $NeuN^+$ and CB^+ neurons shows that SCSC cannot be considered "organotypic" in all aspects. This is not an entirely unexpected finding since these cells are target-dependent for survival through postnatal age. The reaction of glial cells reveals that their activation is limited in both time and space, and nestin expression displays a close resemblance to that described following spinal cord injury. It seems reasonable to propose that SCSC could prove useful in future experiments on the pathophysiology of spinal cord injury although limitations—as in other in vitro models—have to be observed.

Acknowledgements This study was financially supported by the Stiftung Friedrichsheim. S.I.S. received a grant from the Deutsche Akademische Austauschdienst (DAAD). The authors wish to thank Mr. Chalid Ghadban for technical assistance.

References

Albuquerque C, Lee CJ, Jackson AC, MacDermott AB (1999) Subpopulations of GABAergic and non-GABAergic rat dorsal horn neurons express Ca2+-permeable AMPA receptors. Eur J Neurosci 11:2758–2766

Alvarez FJ, Dewey DE, McMillin P, Fyffe RE (1999) Distribution of cholinergic contacts on Renshaw cells in the rat spinal cord: a light microscopic study. J Physiol 515(Pt 3):787–797

Antal M, Petko M, Polgar E, Heizmann CW, Storm-Mathisen J (1996) Direct evidence of an extensive GABAergic innervation of the spinal dorsal horn by fibres descending from the rostral ventromedial medulla. Neuroscience 73:509–518

Bernaudin M, Nouvelot A, MacKenzie ET, Petit E (1998) Selective neuronal vulnerability and specific glial reactions in hippocampal and neocortical organotypic cultures submitted to ischemia. Exp Neurol 150:30–39

Bracken MB (2002) Steroids for acute spinal cord injury. Cochrane Database Syst Rev CD001046

Carlson SL, Parrish ME, Springer JE, Doty K, Dossett L (1998) Acute inflammatory response in spinal cord following impact injury. Exp Neurol 151:77–88

Carr PA, Alvarez FJ, Leman EA, Fyffe RE (1998) Calbindin D28k expression in immunohistochemically identified Renshaw cells. Neuroreport 9:2657–2661

Celio MR (1990) Calbindin D-28k parvalbumin in the rat nervous system. Neuroscience 35:375–475

Chan YM, Wu W, Yip HK, So KF (2002) Development of the regenerative capacity of postnatal axotomized rat spinal motoneurons. Neuroreport 13:1071–1074

D'Orlando C, Fellay B, Schwaller B, Salicio V, Bloc A, Gotzos V, Celio MR (2001) Calretinin and calbindin D-28k delay the onset of cell death after excitotoxic stimulation in transfected P19 cells. Brain Res 909:145–158

Dahlstrand J, Lardelli M, Lendahl U (1995) Nestin mRNA expression correlates with the central nervous system progenitor cell state in many, but not all, regions of developing central nervous system. Brain Res Dev Brain Res 84:109–129

Dusart I, Schwab ME (1994) Secondary cell death and the inflammatory reaction after dorsal hemisection of the rat spinal cord. Eur J Neurosci 6:712–724

Fawcett JW, Asher RA (1999) The glial scar and central nervous system repair. Brain Res Bull 49:377–391

Frisen J, Johansson CB, Torok C, Risling M, Lendahl U (1995) Rapid, widespread, and longlasting induction of nestin contributes to the generation of glial scar tissue after CNS injury. J Cell Biol 131:453–464

Gähwiler BH (1984) Slice cultures of cerebellar, hippocampal and hypothalamic tissue. Experientia 40:235–243

Goodchild AK, Llewellyn-Smith IJ, Sun QJ, Chalmers J, Cunningham AM, Pilowsky PM (2000) Calbindin-immunoreactive neurons in the reticular formation of the rat brainstem: catecholamine content and spinal projections. J Comp Neurol 424:547–562

Greensmith L, Vrbova G (1996) Motoneurone survival: a functional approach. Trends Neurosci 19:450–455

Grossman SD, Rosenberg LJ, Wrathall JR (2001) Temporal-spatial pattern of acute neuronal and glial loss after spinal cord contusion. Exp Neurol 168:273–282

Grossman SD, Wolfe BB, Yasuda RP, Wrathall JR (2000) Changes in NMDA receptor subunit expression in response to contusive spinal cord injury. J Neurochem 75:174–184
Hadley SD, Goshgarian HG (1997) Altered immunoreactivity for glial fibrillary acidic protein in astrocytes within 1 h after cervical spinal cord injury. Exp Neurol 146:380–387
Hailer NP, Grampp A, Nitsch R (1999) Proliferation of microglia and astrocytes in the dentate gyrus following entorhinal cortex lesion: a quantitative bromodeoxyuridine-labelling study. Eur J Neurosci 11:3359–3364
Iacopino A, Christakos S, German D, Sonsalla PK, Altar CA (1992) Calbindin-D28K-containing neurons in animal models of neurodegeneration: possible protection from excitotoxicity. Brain Res Mol Brain Res 13:251–261
Jansen AS, Loewy AD (1997) Neurons lying in the white matter of the upper cervical spinal cord project to the intermediolateral cell column. Neuroscience 77:889–898
Johansson CB, Momma S, Clarke DL, Risling M, Lendahl U, Frisen J (1999) Identification of a neural stem cell in the adult mammalian central nervous system. Cell 96:25–34
Kalman M, Ajtai BM (2001) A comparison of intermediate filament markers for presumptive astroglia in the developing rat neocortex: immunostaining against nestin reveals more detail, than GFAP or vimentin. Int J Dev Neurosci 19:101–108
Kullberg S, Aldskogius H, Ulfhake B (2001) Microglial activation, emergence of ED1-expressing cells and clusterin upregulation in the aging rat CNS, with special reference to the spinal cord. Brain Res 899:169–186
Leme RJ, Chadi G (2001) Distant microglial and astroglial activation secondary to experimental spinal cord lesion. Arq Neuropsiquiatr 59:483–492
Lendahl U, Zimmerman LB, McKay RD (1990) CNS stem cells express a new class of intermediate filament protein. Cell 60:585–595
Li Y, Li H, Kaneko T, Mizuno N (1999) Local circuit neurons showing calbindin D28k-immunoreactivity in the substantia gelatinosa of the medullary dorsal horn of the rat. An immunohistochemical study combined with intracellular staining in slice preparation. Brain Res 840:179–183
Li YQ, Wu SX, Li JL, Kaneko T, Mizuno N (2000) Co-existence of calcium-binding proteins in neurons of the medullary dorsal horn of the rat. Neurosci Lett 286:103–106
Lim SM, Guiloff RJ, Navarrete R (2000) Interneuronal survival and calbindin-D28k expression following motoneuron degeneration. J Neurol Sci 180:46–51
Liu K, Wang Z, Wang H, Zhang Y (2002) Nestin expression and proliferation of ependymal cells in adult rat spinal cord after injury. Chin Med J (Engl) 115:339–341
Liu L, Rudin M, Kozlova EN (2000) Glial cell proliferation in the spinal cord after dorsal rhizotomy or sciatic nerve transection in the adult rat. Exp Brain Res 131:64–73
Magnusson A, Dahlfors G, Blomqvist A (1996) Differential distribution of calcium-binding proteins in the dorsal column nuclei of rats: a combined immunohistochemical and retrograde tract tracing study. Neuroscience 73:497–508
Manitt C, Colicos MA, Thompson KM, Rousselle E, Peterson AC, Kennedy TE (2001) Widespread expression of netrin-1 by neurons and oligodendrocytes in the adult mammalian spinal cord. J Neurosci 21:3911–3922
McMahon A, Wong BS, Iacopino AM, Ng MC, Chi S, German DC (1998) Calbindin-D28k buffers intracellular calcium and promotes resistance to degeneration in PC12 cells. Brain Res Mol Brain Res 54:56–63
Morin-Richaud C, Feldblum S, Privat A (1998) Astrocytes and oligodendrocytes reactions after a total section of the rat spinal cord. Brain Res 783:85–101
Nazli M, Morris R (2000) Comparison of localization of the neurokinin 1 receptor and nitric oxide synthase with calbindin D labelling in the rat spinal cord. Anat Histol Embryol 29:141–143
Notterpek LM, Bullock PN, Malek-Hedayat S, Fisher R, Rome LH (1993) Myelination in cerebellar slice cultures: development of a system amenable to biochemical analysis. J Neurosci Res 36:621–634
Oda Y (1999) Choline acetyltransferase: the structure, distribution and pathologic changes in the central nervous system. Pathol Int 49(11):921–937
Oliveira AL, Risling M, Negro A, Langone F, Cullheim S (2002) Apoptosis of spinal interneurons induced by sciatic nerve axotomy in the neonatal rat is counteracted by nerve growth factor and ciliary neurotrophic factor. J Comp Neurol 447:381–393
Phelps PE, Barber RP, Houser CR, Crawford GD, Salvaterra PM, Vaughn JE (1984) Postnatal development of neurons containing choline acetyltransferase in rat spinal cord: an immunocytochemical study. J Comp Neurol 229:347–361
Popovich PG, Wei P, Stokes BT (1997) Cellular inflammatory response after spinal cord injury in Sprague-Dawley and Lewis rats. J Comp Neurol 377:443–464
Pozzo Miller LD, Mahanty NK, Connor JA, Landis DM (1994) Spontaneous pyramidal cell death in organotypic slice cultures from rat hippocampus is prevented by glutamate receptor antagonists. Neuroscience 63:471–487
Prewitt CM, Niesman IR, Kane CJ, Houle JD (1997) Activated macrophage/microglial cells can promote the regeneration of sensory axons into the injured spinal cord. Exp Neurol 148:433–443
Rabchevsky AG, Streit WJ (1997) Grafting of cultured microglial cells into the lesioned spinal cord of adult rats enhances neurite outgrowth. J Neurosci Res 47:34–48
Ren K, Ruda MA (1994) A comparative study of the calcium-binding proteins calbindin-D28K, calretinin, calmodulin and parvalbumin in the rat spinal cord. Brain Res Brain Res Rev 19:163–179
Ridet JL, Malhotra SK, Privat A, Gage FH (1997) Reactive astrocytes: cellular and molecular cues to biological function. Trends Neurosci 20:570–577
Rintoul GL, Raymond LA, Baimbridge KG (2001) Calcium buffering and protection from excitotoxic cell death by exogenous calbindin-D28k in HEK 293 cells. Cell Calcium 29:277–287
Sahin KS, Mahmood A, Li Y, Yavuz E, Chopp M (1999) Expression of nestin after traumatic brain injury in rat brain. Brain Res 840:153–157
Schmidt-Kastner R, Humpel C (2002) Nestin expression persists in astrocytes of organotypic slice cultures from rat cortex. Int J Dev Neurosci 20:29–38
Schnell L, Fearn S, Klassen H, Schwab ME, Perry VH (1999) Acute inflammatory responses to mechanical lesions in the CNS: differences between brain and spinal cord. Eur J Neurosci 11:3648–3658
Shibuya S, Miyamoto O, Auer R, Itano T, Mori S, Norimatsu H (2002) Embryonic intermediate filament, nestin, expression following traumatic spinal cord injury in adult rats. Neuroscience 114:905
Stoll G, Jander S (1999) The role of microglia and macrophages in the pathophysiology of the CNS. Prog Neurobiol 58:233–247
Streit WJ, Walter SA, Pennell NA (1999) Reactive microgliosis. Prog Neurobiol 57:563–581
Tauer U, Volk B, Heimrich B (1996) Differentiation of Purkinje cells in cerebellar slice cultures: an immunocytochemical and Golgi EM study. Neuropathol Appl Neurobiol 22:361–369
Todd AJ, Spike RC, Polgar E (1998) A quantitative study of neurons which express neurokinin-1 or somatostatin sst2a receptor in rat spinal dorsal horn. Neuroscience 85:459–473
Tzeng SF, Bresnahan JC, Beattie MS, de Vellis J (2001) Upregulation of the HLH Id gene family in neural progenitors and glial cells of the rat spinal cord following contusion injury. J Neurosci Res 66:1161–1172

Wei LC, Shi M, Chen LW, Cao R, Zhang P, Chan YS (2002) Nestin-containing cells express glial fibrillary acidic protein in the proliferative regions of central nervous system of postnatal developing and adult mice. Brain Res Dev Brain Res 139:9–17

Wu Y, Li Y, Liu H, Wu W (1995) Induction of nitric oxide synthase and motoneuron death in newborn and early postnatal rats following spinal root avulsion. Neurosci Lett 194:109–112

Yamamoto S, Yamamoto N, Kitamura T, Nakamura K, Nakafuku M (2001) Proliferation of parenchymal neural progenitors in response to injury in the adult rat spinal cord. Exp Neurol 172:115–127

Yuan Q, Wu W, So KF, Cheung AL, Prevette DM, Oppenheim RW (2000) Effects of neurotrophic factors on motoneuron survival following axonal injury in newborn rats. Neuroreport 11:2237–2241